Received 13 July 2024; revised 15 February 2025; accepted 16 February 2025. Date of publication 27 February 2025; date of current version 28 May 2025.

Compressed Sensing Digital MIMO Radar Using a Non-Uniformly Spaced SIW Sparse Receiver Array

CRISTIAN A. ALISTARH[®] (Member, IEEE), SYMON K. PODILCHAK[®] (Member, IEEE), DAVE J. BEKERS[®] (Senior Member, IEEE), LAURA ANITORI[®] (Senior Member, IEEE), WIM L. VAN ROSSUM[®], ROB BOEKEMA[®] (Member, IEEE), IRAM SHAHZADI² (Student Member, IEEE), MATHINI SELLATHURAI[®] (Fellow, IEEE), JOHN S. THOMPSON[®] (Fellow, IEEE), AND YAHIA M. M. ANTAR[®] (Life Fellow, IEEE)

¹Institute of Sensors, Signals, and Systems, Heriot-Watt University, EH14 4AS Edinburgh, U.K.
 ²Institute for Imaging, Data, and Communications, The University of Edinburgh, EH8 9YL Edinburgh, U.K.
 ³Radar Technology Department, TNO, 2597 AK The Hague, The Netherlands
 ⁴Department of Electrical and Computer Engineering, Royal Military College of Canada, Kingston, ON K7K 7B4, Canada

CORRESPONDING AUTHOR: S. K. PODILCHAK (e-mail: s.podilchak@ed.ac.uk)

This work was supported in part by the European Union's Horizon 2020 Research and Innovation Programme through the Marie Sklodowska-Curie under Grant 709372, in part by the Engineering and Physical Sciences Research Council through Project Large Scale Antenna Systems Made Practical: Advanced Signal Processing for Compact Deployments under Grant EP/M014126/1 and through the Project Low-complexity processing for mm-Wave massive MIMO under Grant EP/P000703/1, and in part by the European Microwave Association (EuMA) under the EuMA Internship Award.

ABSTRACT A compressed sensing (CS) digital radar system based on a sparse array design is proposed for use in automotive collision-avoidance applications. The proof-of-concept radar system offers an enlarged antenna aperture, employing fewer elements and can distinguish targets at an angular separation of only 2 degrees for a bandwidth of 6.25%. This resolution is made possible using a multiple-input multiple-output (MIMO) configuration from the original sparse array which was implemented and tested using substrate integrated waveguide (SIW) technology. More specifically, the total aperture size (of the effective virtual receiver array) is 23.5λ which is equivalent to a uniform-linear array (ULA) having 48 elements spaced at 0.5λ apart. However, the total number of elements is 32. This defines a cost-effective setup offering a reduction of 16 elements which accounts for a 33% reduction in the number of required channels for the SIW array. Also, the radar exploits sparse-reconstruction techniques for target detection. Results of the simulations and measurements show that the performance of the proposed SIW antenna and experimentally verified radar system can offer competitive high-resolution detection when compared to other findings in the literature and to the best knowledge of the authors, no similar antenna and radar system implementation has been designed and experimentally verified.

INDEX TERMS Compressed sensing, digital beamforming, frequency modulated continuous wave (FMCW), short-range radar (SRR).

I. INTRODUCTION

RADAR detection for autonomous vehicles has seen a proliferation in recent years, with industries and governments investing heavily in the progress of these systems. While the industry has reduced the growth in 2020 by 21%, it is still projected that the radar industry will grow in the foreseeable future [1]. Also, radar systems have become more complex and have reached a certain maturity, with the topics being directed to microwave and millimetre-wave systems and complex RF processing

chains [2]. Market trends for the automotive radar industry are also influenced by performance safety programmes, such as the European New Car Assessment Programme (EuroNCAP) [1]. Moreover, EuroNCAP has set standards for automatic emergency breaking (AEB) for collision avoidance systems since 2014.

The latest AEB systems, for example, should be able to avoid crashes for vehicles coming from the side of the car at a field-of-view (FOV) of 120° on each side and for a distance of 150 m [1]. The front looking radar should also be capable

Reference	Carrier Freq. (GHz)	Receiver Array Architecture	Antenna Type	Equivalent Receiver Array (ERA)	HRSP Method (SSP) in the Angular Domain	Receiver Percentage Bandwidth	Range Resolution (cm)	Angular Resolution as RCW or λ/D
[19]	10	ULA MIMO	Planar array of microstrip patches	18 (= 2×9)	Fourier, BPDN (LASSO / L2 / L1) by SPGL1	16%	9.3	6.4°
[4]	76	Sparse virtual irregular array by MIMO and ULA	Planar array of microstrip patches	12 (= 3×4)	OMP, BPDN by SPGL1 FOCUSS	1.3%	15	6.6° (sparse) 11.8° (ULA)
[20]	76.5	Regular virtual array by MIMO	Planar array of microstrip patches	32 (= 4 × 8)	IMAT	2.62%	7.5	2°
[7]	300	Single element with mechanical movement	Horn Antenna	5 TX-RX channels	Bilateration, backprojection, elastic net	6.2%	0.0083	1.13°
This work	24	Sparse virtual array by MIMO	SIW-fed planar slot array	32 $= 4 \times (4 \times 2)$	Dual formulation of BPDN by YALL1	6.25%	10	2°

TABLE 1. Comparison of other automotive radar system performances and our work.

to operate over a FOV of at least 20° and permit detection of objects up to a range of 250 m. In addition, since 2018, radars are required to be able to avoid cyclist crashes from the side and front of the car [1]. This capability is possible only if the elevation information is retrieved from the environment. Therefore, the latest radar systems require detection in four dimensions (4D radar): range, Doppler, azimuth, and elevation. In addition to this, the manufacturing of the sensors must be cost-effective and practical for mass production [3].

To meet these general design goals, hardware developments in automotive radar have also progressed in recent years. One point of interest for microwave and millimetre-wave radar systems has been directed towards enhanced resolution of targets and the integration of digital technologies [2]. Also, a frequently mentioned benefit of sparse-signal processing (SSP) is the possible resolution improvements as compared to traditional-signal processing (TSP), and potentially, lower hardware costs. Moreover, SSP with various algorithmic solutions has been shown to have improved resolution probability as compared to TSP [4], [5], [6], [7], [8], [9]. Also, applying reprocessing on the same data after detection with low sidelobes, one may consider to perform pre-whitening in order to improve accuracy [10], [11], [12].

Given this stage in the developments and depending on system requirements, a radar may need high resolution in some or all dimensions. Our approach in this work is to focus on azimuth resolution as well as reduced hardware requirements by exploiting sparsity, but the approach can also be applied to the elevation and range dimensions, netted radars [13], [14], [15], [16], and other sectorized systems [17]. In particular, [17] demonstrated a sectorized

and modular MIMO radar system which was capable of distinguishing targets at $\pm 2^{\circ}$ in angular separation for the azimuth domain.

A new study is reported in the following, which chooses the optimal MIMO antenna element spacing mainly focusing on achieving the best possible half-power beamwidth (HPBW) and sidelobe level (SLL) performance. Moreover, our approach in the receiver (RX) antenna design is to determine the appropriate sparse configuration by thinning a pre-specified regular array with spacing $\lambda/2$. The main criterion in determining this configuration is based on the HPBW of the resulting virtual array at the receiver. More specifically, this 32-element MIMO radar antenna configuration achieves a virtual aperture length of 23.5 λ , and this is equivalent to a 48-element ULA with $\lambda/2$ spacing resulting in a 33% reduction in the number of elements.

This can offer significant operational cost savings for the radar as each element is typically connected to an RF channel which can be digitized, and the reduction in the number of elements can enable reduced power and hardware requirements. Also, when our proposed array is compared to an equivalent ULA with $\lambda/4$ spacing (which would require 95 elements for the same aperture length), our antenna system demonstrates a 66% reduction in the number of elements. Nevertheless, our developed sparse array based on $\lambda/2$ element spacing was manufactured using substrate integrated waveguide (SIW) technology, and experimentally tested and built-up with a set of frequency-modulated continuous waveform (FMCW) target studies defining an experimental and modular digital MIMO radar.

This experimental and proof-of-concept radar system is advantageous; i.e., detecting two targets with a 2° separation

with a bandwidth of more than 6% (see Table 1). Another unique and novel feature of the proposed MIMO radar is the spectral smoothing [18] added to the SSP, which is shown to offer improved SNR performance. To our best knowledge, no similar antenna and radar system has been reported previously offering improved target-separation resolution capability.

The paper is organized as follows. In Section II we discuss the literature of SSP in the context of automotive radar and sparse arrays. In Section III we describe the employed CS approach for the digital radar system trials. In Section IV the sparse antenna design is outlined and its performance is assessed. In Section V we present the simulation and measurement setup of the CS digital radar system. A conclusion follows in Section VI.

II. LITERATURE OF AUTOMOTIVE RADAR SYSTEMS

There have been significant advancements in RF electronic components and radar systems while exploiting fully digital transmit-receive antenna arrays. These advances can be observed in the literature in the context of new radar systems. Moreover, there has been significant development in sparse arrays, MIMO, and SSP for automotive radar and other related applications. This is because such architectures can lead to reduced sampling requirements and data rates, while maintaining angular resolution. As a result, innovative proof-of-concept systems have been designed and presented in the literature as described next.

An example is the fully digital X-band FMCW radar system described in [19], [21]. A linear array of 12 folded dipoles was distributed in two transmit (TX) subarrays (the outer two elements on both sides) and one receive (RX) subarray (the 8 center elements). The spacing within the subarrays approximates $\lambda/2$, while the spacing between (outer elements of) the subarrays approximates $\lambda/4$. With this configuration, a virtual array of 18 elements was formed by MIMO techniques, whose spacing is $\lambda/4$ when considered 2-way Tx-Rx [21, Fig. 2] and, hence, the 2-way Rayleigh-cell (λ/D) width (i.e., RCW) is 12.7°, while 1-way it is 6.4°. The radar processing exploited matched filtering (MF) and MUSIC.

Another contribution aimed directly at automotive radars is [4]. Similar to [21], the paper describes the formation of a virtual array of 29 elements with half-wavelength spacing, by MIMO techniques, and the application of five high-resolution processing methods [4]. Additionally, several types of thinned virtual arrays are considered and results in [4] report the smallest target separation of more than two Reyleigh cells of the virtual array (8.6° in [4, Fig. 5 (right)] versus 3.95°). In [4] also, an analysis of resolution is presented. For example, as [4, Fig. 4 (middle)] shows, three high-resolution methods applied to a virtual aperture of 8.64λ with 12 elements (with optimized positions) can resolve two targets. This research was extended in [6] where an antenna positioning scheme for CS-MIMO radar was reported.

The work in [20] is also aimed at 77 GHz automotive radar applications. The paper describes the synthesis of a

sparse array by thinning a regular, Nyquist-sampled, array using a genetic algorithm and such that the irregularity of the obtained array prevents side-lobe rise due to the increased spacing between the antenna-array elements. The missing array elements are reconstructed by inter- and extrapolation using the iterative method with adaptive threshold (IMAT) algorithm. This procedure lowers potentially sidelobes further and it narrows the beamwith since the aperture is almost doubled in extent. Generally, the SNR is not increased by the reconstruction. The Rayleigh cell of the resulting (virtual) array of length $29\,\lambda$ is 2.0° .

The work in [7] is more challenging from a manufacturing point-of-view given a carrier frequency of 300 GHz. It discusses target localisation by a 300 GHz system, whose angular Rayleigh cell is $1^{\circ}/0.886 \approx 1.13^{\circ}$. The considered signal-processing methods are bilateration, back-projection, and HRSP by elastic net. They are applied to a measurement with two targets separated in elevation by 3.4°. So, the targets are separated by approximately three Rayleigh cells. Another contribution in [22] examined the influence of coupling on the virtual array positions of a MIMO radar and a calibration method using the Discrete Fourier transform (DFT) for antenna element positioning.

These contributions are summarized and compared in Table 1 and show that academia and industry are seeking compact and modular automotive radar systems. Such systems should exploit planar implementations as well as cost effectiveness whilst being scalable to larger radars. This combination brings up clear requirements and system characteristics: high resolution for small to moderate aperture sizes, and with reduced digital hardware requirements. Moreover, the comparisons in Table 1 suggest that the proposed sparse MIMO array design and experimentally tested radar can offer improved system performances (i.e., increased angular resolution achieving 2° target detection with a bandwidth of 6.25%), while other uniform MIMO and ULA solutions may achieve reduced metrics. To the best knowledge of the authors, no similar SIW antenna array and digital FMCW radar system using SSP has been demonstrated previously.

III. SPARSE PROCESSING

According to the Nyquist-Shannon Theorem, any band-limited signal can be reconstructed without ambiguities if this signal is sampled with at least twice the bandwidth frequency. While this is simple and effective, it also adds a data surplus to the analogue-to-digital conversion process. It would be more efficient to extract only the relevant information from the detection, by employing compressive sensing (CS) in order to detect and classify the targets, and so, reducing the signal processing requirements.

Presuming that pulse compression has been carried out and focusing on a specific range bin, we can describe the received signal by

$$\mathbf{y} = \sum_{i=0}^{K} \mathbf{a}(\theta_i) \, x_i + \mathbf{n} = \mathbf{A}\mathbf{x} + \mathbf{n} \tag{1}$$

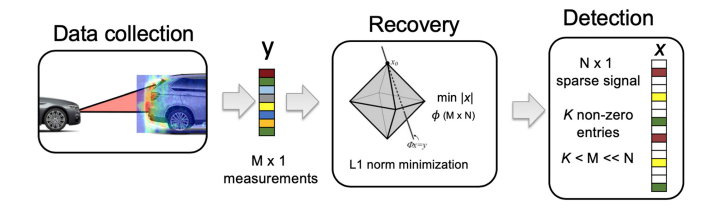


FIGURE 1. Diagram showing the steps that can be taken to apply CS reconstruction in an automotive radar scenario.

where x_i are complex amplitudes, $a(\theta_i)$ are the responses to unit sources at different angles, y contains the received signal samples, n is the noise, and A is the sensing matrix or dictionary. Aiming at enabling high-resolution data processing based on a single snapshot (in the angular domain), we formulate the well-known least-squares problem penalized or regularized by the ℓ_1 -norm,

$$\hat{x} = \underset{x}{\operatorname{argmin}} \|x\|_{1} + \frac{1}{2\mu} \|y - Ax\|_{2}^{2}. \tag{2}$$

This minimization problem is the Basis Pursuit Denoising (BPDN) problem or the Langrangian formulation of the Least Absolute Shrinkage and Selection Operator (LASSO). It presumes sparsity of the 'solution vector' x. The variable μ in (2) represents the weighting or regularization parameter. A theoretical analysis of the choice of μ can be found in [23] and an approach to set μ by requiring a certain falsealarm rate in noise-only simulations can be found in [11]. For target situations, one can get insight into the optimal algorithm settings by considering the so-called sparsity-SNR phase transition diagrams. Such diagrams represent detection or failure rates for varying numbers of targets and varying SNR. In [24] such diagrams are generated and studied for simulated data and for measured data of realistic traffic scenarios.

It should be mentioned that there are two basic needs for CS: recoverability and stability. With recoverability, the point of interest is the types of measurements and their number to extract a sufficiently sparse signal. Stability refers to the robustness of the algorithm over time and noise variation [25]. Basically, with a known measurement y, it can be assumed that a reconstruction algorithm will look at the sparsest solution for the measurement samples. An illustration of the CS reconstruction steps is shown in Figure 1, showing data acquisition, sparse data formation and reconstruction using l_1 minimisation.

A fast and robust method of performing sparse recovery based on Eq. (2), can be obtained by rewriting this objective to its dual form, see [26, Sec. 2.3]. This form can be approximated numerically by an Alternating Direction of Multipliers Method (ADMM), as developed in [27], [28]; i.e., see the ADMM-based iteration scheme in [26, eq. (2.26)] for the relevant orthonormal dictionary developed. This scheme is implemented in the YALL1 toolbox for sparse reconstruction for both orthonormal and

non-orthonormal dictionaries. See also the (L1/L2) problem in [29, p. 1].

These sparse-reconstruction techniques are important in modern radar signal processing and can enable enhanced resolution while reducing hardware requirements and radar system complexity. In our approach adopted herein, we utilize the LASSO formulation to enforce sparsity in the angular domain. This allows for accurate target detection and with minimal antenna elements. To solve this problem, we employ ADMM, which is particularly well-suited for largescale, constrained optimization problems [27], [28]. ADMM iteratively decomposes the problem into smaller, manageable data sets (or updates), ensuring fast convergence and robustness against noise. More specifically, ADMM operates by splitting the overall objective into sub-problems which are then tackled individually, using an augmented Lagrangian framework to enforce consensus between variables. In each iteration, ADMM alternates between minimizing a smooth loss term (e.g., least-squares data fidelity) with respect to one set of variables, and minimizing a potentially nonsmooth term (e.g., the L1 penalty) with respect to the previous set [27], [28]. The resulting dual variables are then updated to reconcile the solutions from these two steps, effectively imposing the equality or "consensus" constraints.

It is interesting to note that an implementation of ADMM on chip was described in [30], which may ease the integration of ADMM for automotive applications. This decomposition strategy allows ADMM to handle large-scale or high-dimensional problems more efficiently than many competing methods. In YALL1 moreover, ADMM is implemented in a way that accommodates both orthonormal and non-orthonormal dictionaries seamlessly, offering a flexible framework for sparse recovery. Through its iterative updates and ability to handle non-smooth regularizers like the L1 norm, ADMM in YALL1 converges reliably to a sparse solution [26], [27], [28], [29], and this can offer efficient and robust (sparse) radar signal processing.

In general, YALL1 requires a few iterative steps to find the reconstructed vector x which is k-sparse. A flow diagram depicted in Fig. 2 shows the procedures taken in the algorithmic process. It is also important to initialize the target vector and the YALL1 parameters appropriately. These parameters refer to the noise threshold, maximum number of iterations, etc. These parameters have been summarized in Table 2 for the results of this paper. Setting the parameters for YALL1 is important since its convergence depends on setting adequate parameters. In the iteration phase of the algorithm as shown in Fig. 2, the method for obtaining the reconstructed signal is achieved by using minimized Lagrangian functions through an alternating minimisation procedure and an update of each multiplier after each sweep.

¹In the latter case, the update of the dual variable y in the iteration scheme is replaced by [26, eq. (2.23)]. Note also that, in the YALL1 toolbox, the parameter β is set equal to 1.

FIGURE 2. Your Algorithm for L1 (YALL1) procedure diagram.

TABLE 2. YALL1 input value parameters.

Parameter	Range	Description		
		This parameter assigns		
ρ	(1e-2;1e-3)	the L1/L2 model, usually with		
		a positive value.		
w	(0;1)	YALL1 can compute		
.,	(0,1)	the conversion with non-uniform weights.		
δ	0.1	Noise level threshold		
Print	[0,1,2]	Levels of printout		
Maxit	[0:9999]	Maximum iterations		
ν	[0:1]	> 0 for L2/L1 model		
ρ	1e-3	> 0 for L2/L1 model		
nonneg	0	1 for non-negativity		
μ	set by user	penalty parameter		

This methodology solves this convex optimization problem by dividing it into smaller pieces which are simpler to solve.

In this paper we will use the aforementioned ADMM implementation of YALL1 for our high-resolution (HR) radar signal processing. It should be noted that we have considered other HR methods in [31], namely MVDR/CAPON, MUSIC, and Functional Projection whilst considering standard $\lambda/2$ element spacing at the radar receiver; i.e., a non-sparse antenna array. In particular, the radar setup in [31] demonstrated an angular resolution of at least 12.6° for a 2TX 4RX experimental FMCW radar setup. Other studies for different virtual MIMO aperture sizes have also been reported in [17] considering DAS target detection. For our reported results in the following sections, which adopt a newly designed and sparse MIMO antenna array (see Section IV), we use the aforementioned (L1/L2) problem implementation in YALL1. These efforts are then experimentally demonstrated for the first time in a radar system demonstration achieving 2°



FIGURE 3. Template for obtaining a sparse array design for a 2TX 4RX receiver MIMO array, with ½ inter-element spacing.

angular resolution for a bandwidth of 6.25% (see Table 1, and Section V). Moreover, the dictionary employed for our SPP is an oversampled collection of linear phase tapers, by which the vector \mathbf{x} is sparse for a limited number of targets in the angular domain.² Because of the oversampling in the dictionary, the non-orthonormal dictionary option of YALL1 is adopted. Also, the dictionary columns are normalized to have unit 2-norms, otherwise convergence problems may arise. The weight parameter μ (ρ in the YALL1 implementation), the convergence tolerance, and the algorithm tuning parameter γ are fixed to 0.01, 5·10⁻⁶, and 0.99, respectively. Also, the maximum number of iterations is 9999.

IV. SPARSE ANTENNA ARRAY DESIGN AND RESULTS

There has been a wide interest in sparse antenna array design for automotive radar systems due to the capability of obtaining a larger aperture and modeling SLL for better target detection [2], [4], [7]. While most works use different algorithms to obtain the optimal solution based on a set of constraints (antenna size, number of elements, desired SLL, etc.), our work starts with a standard $^{\lambda}/_{2}$ -spaced array, and then, makes it sparse. This approach is simple and develops a clear methodology of how to obtain an optimal MIMO sparse array.

A. DESIGN CONSIDERATIONS FOR THE SPARSE ARRAY & ANALYSIS

As described in Section I, the radar receiver antenna considered in this work employs substrate integrated waveguide (SIW) technology. A $^{\lambda}/_{2}$ inter-element spaced element version has already been fabricated and tested in [32] considering some preliminary radar trials. Each element of the array is realized by a series-fed (linear) sub-array of three slots for radiation. The far-field pattern for this sub-array element can be seen in Fig. 12, from [17]. In our newly proposed sparse array design, this same SIW sub-array element was also employed. The new design methodology is as follows. We first thin an eight-element receiver array to form a sparse four-element array while considering a similar SIW sub-array transmitter. Next, a second transmitter

²Consequently, the sparsifying weight-matrix W in the YALL1 (L1/L2) implementation is the identity. Also, no weights in the ℓ_1 -norm are introduced according to [29, eq. (9)], since no specific angles are promoted.

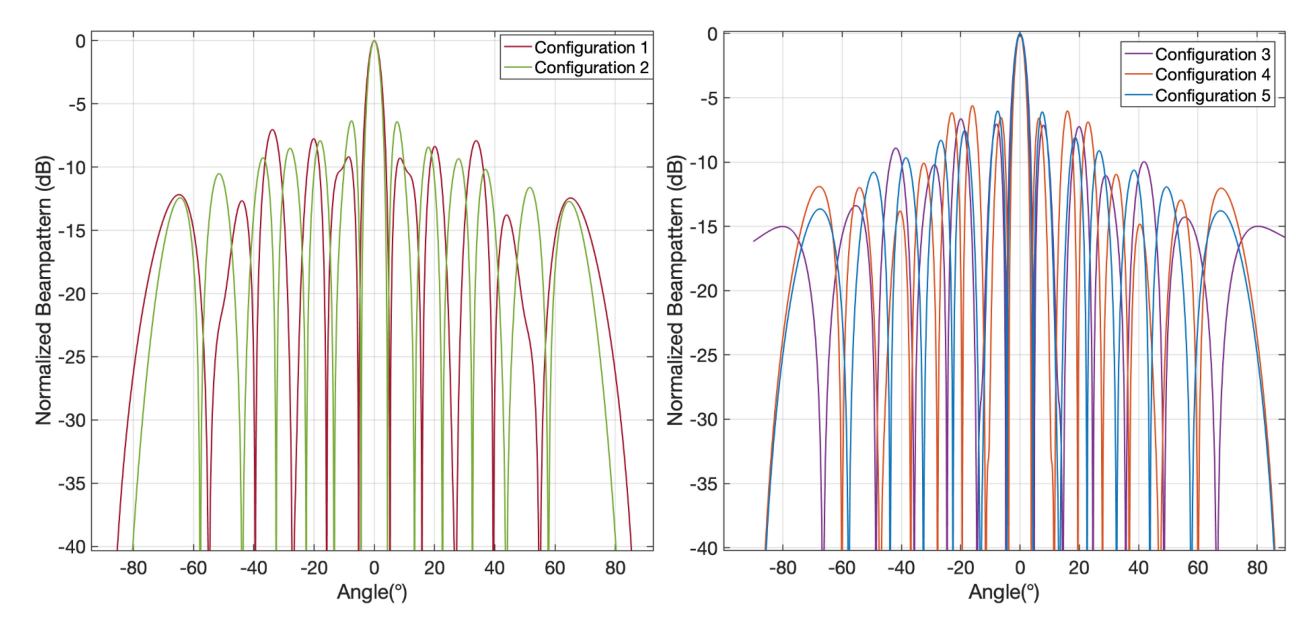


FIGURE 4. Numerically calculated azimuth beam patterns using the element-beam pattern multiplied by the array factors of the configurations listed in Table 3.

is included forming a virtual receiver aperture which is also sparse.

It should be mentioned that an exhaustive search was carried out for the possible array configurations, by changing the separation between the transmit elements (see Fig. 3). The motivation was to achieve the best possible half-power beamwidth (HPBW) and SLL. Figure 3 also illustrates the baseline MIMO antenna system with 2TX and 4RX, which was then made sparse. By varying the spacing between the two antenna transmitters it allows for the creation of a larger virtual antenna receiver with 8 elements (2×4) , which can increase the total aperture length and reduce the HPBW. This reduction can improve the radar target resolution. However, this extra degree of freedom comes with the possibility of introducing grating lobes and raising the SLL, which are undesirable. Basically, in our sparse array design we are aiming to minimize these peak SLLs when compared to the main beam.

While it might be better to vary the inter-element spacing non-uniformly as in [17], it is desired in this study to show that a high angular resolution can also be achieved while starting with a simple equidistant interelement spacing. This starting point helps convergence to the best solution in our evaluations in terms of narrowest HPBW and low SLL. In particular, an exhaustive two-stage study was completed where the HPBW was the primary criterion for the array while the SLL was secondary. See Table 3, where the five best configurations are reported, while Fig. 4 presents a comparison of the different patterns. As mentioned previously, these configurations were gathered by first discovering the best solution for the individual MIMO antenna array, mainly by, selecting different elements which were then driven within each sub-array tile and by varying the spacing between the sub-arrays (see Fig. 3),

TABLE 3. Comparison of the five best sparse (receive) antenna array configurations.

Config.	Inter-array	Element Positions (λ)	HPBW	SLL
Nr.	spacing (λ)	Element Fositions (X)		(dB)
1	7.5	-2, 0, 1, 1.5, 5.5, 7.5, 8.5, 9	3.6°	-5.23
2	7	-2, -1, 0, 1, 5, 5.5, 7, 8	4.0°	-5.06
3	6.5	-2, -0.5, 0, 1, 4.5, 5.5, 6, 8	4.0°	-6.17
4	6	-2, -1, 0, 1, 4, 5.5, 6, 7	4.4°	-5.86
5	5.5	-2, 0, 1, 1.5, 3.5, 5.5, 6.5, 7	4.6°	-5.00

Note: the actual array is located between -2λ and 1.5λ and the eight-element virtual array is next to it. Note that, here, λ is the free-space wavelength, which is 1.25 cm in free space at 24 GHz.

whilst aiming for best possible performance for the total MIMO sparse array. This was defined by narrow HPBW and low SLLs.

The u-v response in Fig. 5 helps to even more observe the SLLs when varying the antenna scanning angle and the representation of the simulated response for array configuration #1 (as defined in Table 3), and can be observed in Fig. 5. We choose the coordinate system as follows. The z-axis is directed along the array axis, the x-axis is directed perpendicular to the antenna plane, and the y-axis is directed along the slots of a single element such that a right-handed coordinate system is obtained. Consequently, the xz-plane is the azimuth plane and the yz-plane is the elevation plane. Next, we introduce a classical spherical coordinate system and a corresponding uv-coordinate system with $u = \sin \theta \cos \phi$ along the y-axis and $v = \sin \theta \sin \phi$ along the z-axis. We consider the radiation pattern in the azimuth

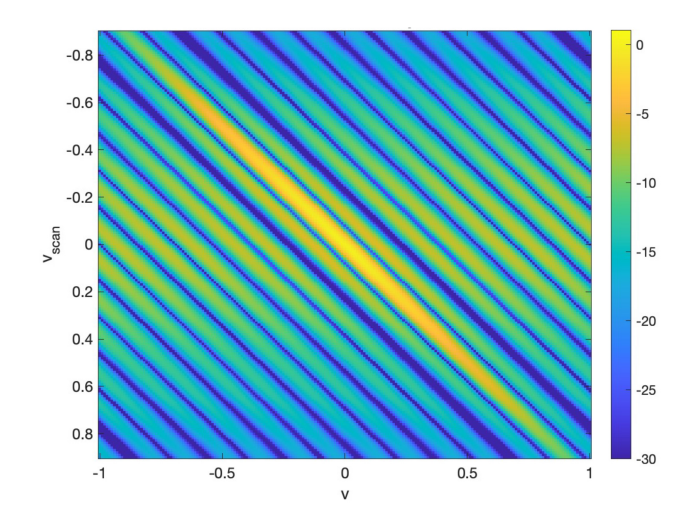


FIGURE 5. Calculated response for the eight-element (receive) antenna array in (u)v-coordinates for a complete scan by configuration #1 in Table 3 in the plane v = 0. Here, $v = \sin \theta$ and $v_{\text{scan}} = \sin \theta_{\text{scan}}$, and θ and θ_{scan} are the observation and as the scan angles in a plane that incorporates the array axis. The response is calculated as the simulated element pattern (of the four slots) and the array factor.

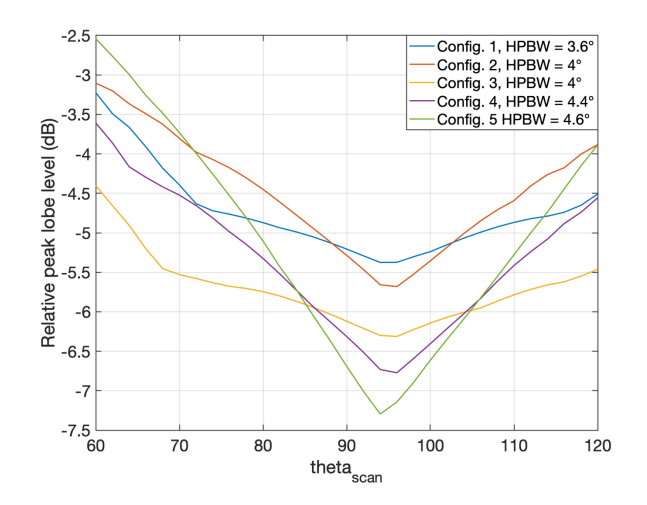


FIGURE 6. SLL comparison for the different virtual array receiver configurations as described in Table 3. The broadside HPBW is also defined in the legend.

plane u = 0 or $\phi = \pi/2$. As can be observed in Fig. 5, a maximum SLL of about -4 dB is achieved. Even if the SLL is under a certain margin when scanning at different angles, it is also possible to have other side-lobes in a different plane. Sweeping the θ angle allows the detection of these

Figure 6 also reports the SLL variation with scanning angle for all configurations highlighted in Table 3. This graph shows the SLL variance with steering antenna angle, and it can be observed that at 30° off broadside the SLL can rise to -2.5 dB. This indicates that the antenna array should not be used for beamsteering in certain cases, as the target detection may see false targets. In these situations, it is possible to add tapering to reduce the SLLs at the expense of HPBW and this is possible with more advanced digital radar antenna implementations. Regardless, from this graph it can be seen that configuration #3 provides the best SLL over

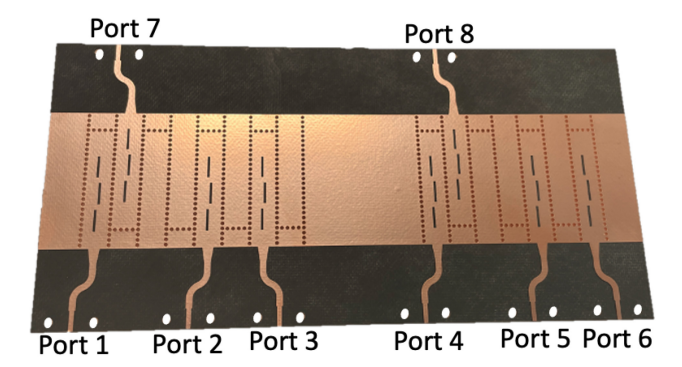


FIGURE 7. Manufactured sparse SIW radar antenna with improved HPBW as compared to an 8-element array with half-wavelength spacing.

scan angle and this is the one which has been down-selected for fabrication.

An alternative approach of selecting element positions for MIMO radars within an automotive scenario was presented in [6]. That work was based on the minimization of the mutual coherence of the sensing matrix, and Monte Carlo simulations demonstrated that the optimized 3TX and 4RX array outperforms other more standard arrays with a similar number of elements. In contrast to our discrete selection problem with minimum HPBW and SLL as the objective, element positions were continuously optimized with minimum coherency of the sensing matrix as the objective in [6]. The optimization result is listed in [6], Section III, and the array pattern (and hence the SLL) is determined a posteriori for that work. See also Fig. 3 in [6] for more details where antenna performance values are comparable to the ones reported for our newly proposed SIW design, as further described next.

B. MANUFACTURED ANTENNA ARRAY & RESULTS

Microstrip arrays have been extensively used for automotive radar systems since this type of antenna is simple to design and easy to manufacture [33]. However, radiation losses of substrate-integrated waveguide (SIW) antennas are significantly reduced for millimetre-wave frequencies when compared with microstrip patch antennas [34], [35]. Also, SIW-type antenna arrays are generally less dispersive when compared to microstrip structures and other patch-type arrays [36], leading to reduced beam-squint over frequency which is generally desired for improved radar accuracy. This is because SIW technology supports the fundamental and dominant TE_{01} -like mode, and this field profile is known to have lower dispersion when compared to the quasi-TEM mode of microstrip [36], [37]. Moreover, since the transmission frequency is constantly being changed in an FMCW radar, the beam angle can vary due to this dispersion and when employing more standard microstrip-based antenna arrays, this dispersive property is undesirable in radar detection [17].

Following these previous developments, SIW technology has been selected for our radar antenna (see Fig. 7). The antenna, configuration #3 from Table 3, was manufactured

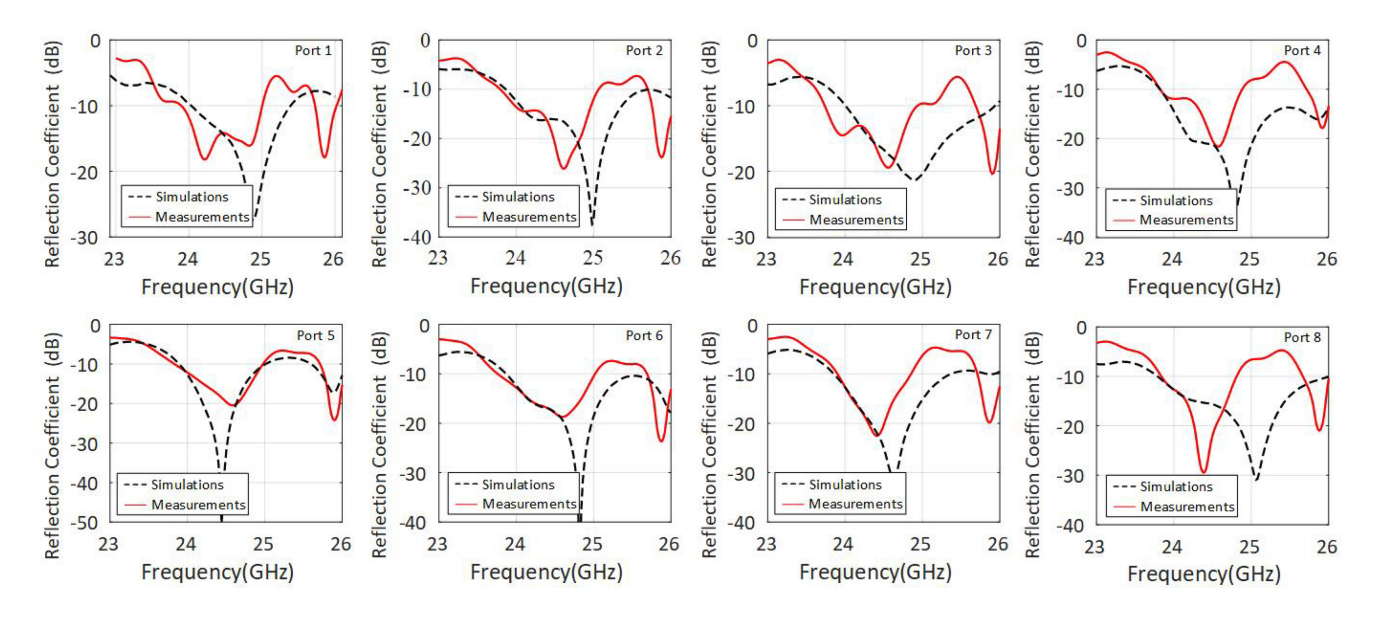


FIGURE 8. Simulated and measured reflection coefficient values for the manufactured SIW sparse 8-element antenna array (see Fig. 7).

using Rogers Duroid 5880 and for operation at 24 GHz by following [17]. Also, the via diameter, pitch and waveguide width were chosen according to the design guidelines in [38]. The dimensions and positioning of the slots was then optimized with the aid of design equations as found in [39] as well as the commercial full-wave simulation software CST. It should also be mentioned that the array was designed for 24 GHz, but could easily be up-scaled for higher carrier frequencies and operation at 77 GHz, for example.

For feeding the antenna prototype, a microstrip-to-SIW transition was employed and utilized a tapered section for improved matching. Simulated and measured reflection coefficient values for the fabricated SIW sparse antennaarray (see Fig. 7) are reported in Fig. 8. A reasonable agreement between simulations and measurements can be observed, particularly for the frequency range up to 25 GHz. Most importantly, the -10 dB impedance band from about 24 GHz to 25 GHz for the manufactured SIW array is well predicted by the simulations. There is some minor disagreement between the position of the reflection coefficient minimums, which could be related to some minor connector misalignment or change in the rated value of the dielectric constant which was specified by the manufacturer at 10 GHz (similar challenges were documented in [40], [41] and references therein). Regardless of these practicalities, the developed SIW radar antenna is well matched from about 24 to 25 GHz.

For beam pattern measurements, the antenna under test (AUT) was placed at 2.5 m from a standard reference horn in the far-field and gain values were determined as a function of angle. Simulations and measurements are shown in Figs. 9 and 10 for the azimuth and elevation planes, respectively. A fan beam pattern is observed in the elevation plane to illuminate targets for the application scenario of

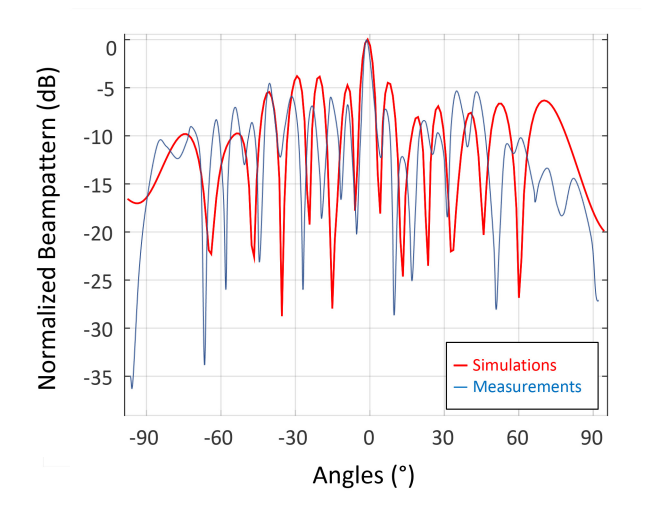


FIGURE 9. Azimuth beampattern for the 8-element SIW receiver (see Fig. 7).

automotive radar, while a directive beam is shown in the azimuth plane supporting target resolution.

It should be mentioned that there is a general agreement between the simulations and measurements, with some minor discrepancies typical at microwave/millimeter-wave frequencies. These can be attributed to minor fabrication and connector practicalities (as mentioned above) and/or some interaction between the antenna under test and the plastic mounting platform. Regardless, the measured SLL is at about -5 dB below the main beam peak which is consistent with the simulations. The measured realised gain maximum for the SIW radar antenna is 16.7 dB, only 0.7 dB below when compared to the simulated value of 17.4 dB. In addition, the simulated total antenna efficiency (including connectors) is 83.5%. The measured cross-polarization levels (all results not

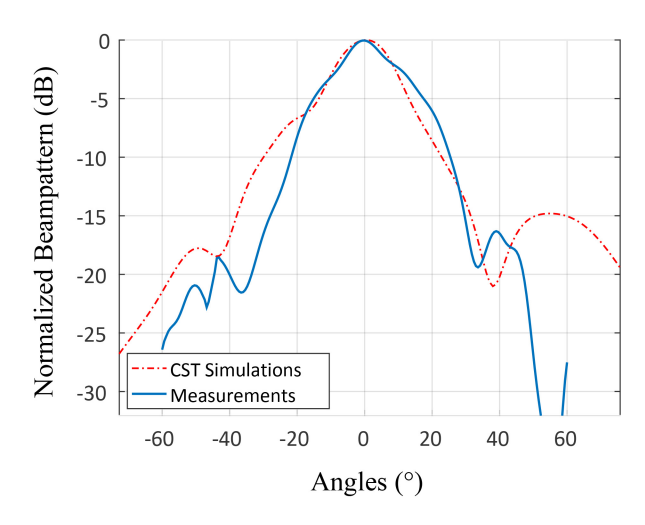


FIGURE 10. Flevation beampattern for the 8-element SIW antenna receiver.

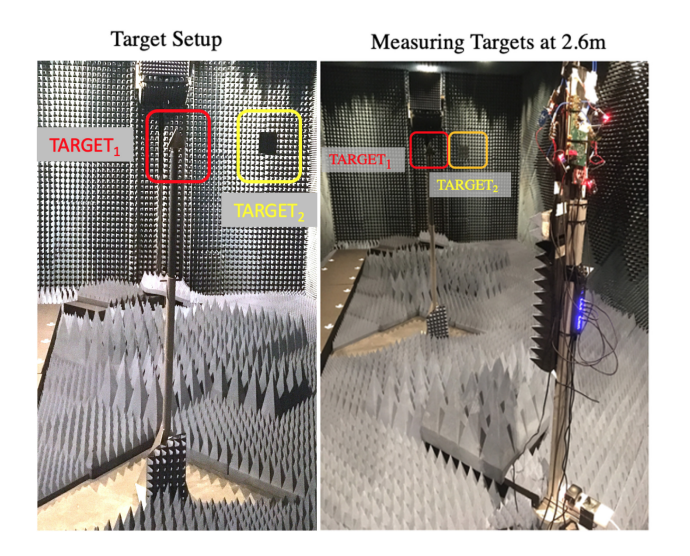


FIGURE 11. Hardware setup for target detection measurements comprising the two targets positioned at 2.6m from the FMCW radar demonstrator system.

shown for brevity) are also in agreement with the simulations being more than 20 dB below the main beam maximum at broadside.

V. TARGET DETECTION AND RADAR SYSTEM RESULTS

A photograph of the digital FMCW radar system demonstrator is shown in Fig. 11. The radar electronics are defined by monolithic microwave integrated circuits (MMICs) as described earlier in [17]; i.e., an ADF5901 MMICtransmitter, the ADF5904 receiver, and the ADF4159 phase-locked loop.

Two targets have been selected to simulate target detection in an automotive radar collision avoidance scenario. This detection trial is meant to simulate the case where a car would be represented with two targets close by. If for example the car would be able to detect only one of the targets, then it would not be sufficient in certain situations to avoid a collision. Hence it is important to perform this trial in a controlled environment such as an anechoic chamber. The

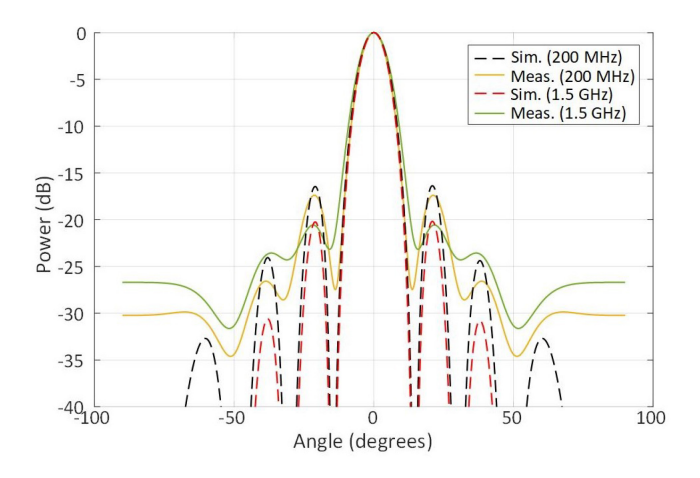


FIGURE 12. Normalised target return for frequency calibration at 200 MHz and 1.5 GHz for a corner reflector with 10 cm size.

two selected targets are an aluminum corner reflector with an edge size of 10 cm on each side and a metal plate with an edge also of 10 cm. In our study we selected targets with similar sizes to detect them at a close angular spacing using the CS and SSP approaches outlined earlier in Section III.

Prior to two-target testing, a preliminary study was completed to assess the radar system bandwidth whilst using a more standard (non-sparse), eight-element (2Tx, 4Rx) $\lambda/2$ spaced MIMO receiver. The angular pattern of this study after pulse compression can be seen in Fig. 12 to assess the SLL for a single-target while also ensuring channels imbalances were corrected for the digital radar. As can be observed, the SLLs for the 1.5 GHz measurements were improved compared to the 200 MHz bandwidth system and results are consistent with simulations. Given these findings, the radar system was set with a bandwidth of 1.5 GHz as in [17], and was used for the detection trials. Also, during system testing, precision-controlled linear stages (with low reflectivity) were used to position targets with high accuracy; i.e., laser guided, while environmental factors were carefully monitored to ensure measurement consistency and limited system drift.

A. RADAR SYSTEM TESTING

For the two-target studies, a square target plate was placed at a fixed position in the anechoic chamber, while the corner reflector was attached to a plastic pole which allowed its spatial positioning for the detection trials. The measurement setup is shown in Fig. 11 with indicated target positions. The targets were positioned in the middle of the anechoic chamber at 2.6 meters from the radar system demonstrator using the SIW sparse antenna array outlined in Section IV. The radar hardware is also shown, attached to a third pole and was formed by using a four-tiled version of the developed SIW antenna defining the modular implementation. This setup realized the prototype proof-of-concept radar system comprised of 32 elements (= $4\times(4\times2)$) for the effective virtual receiver array. A similar procedure was reported in [17] by some of the authors for a sector-based FMCW-MIMO radar. That system

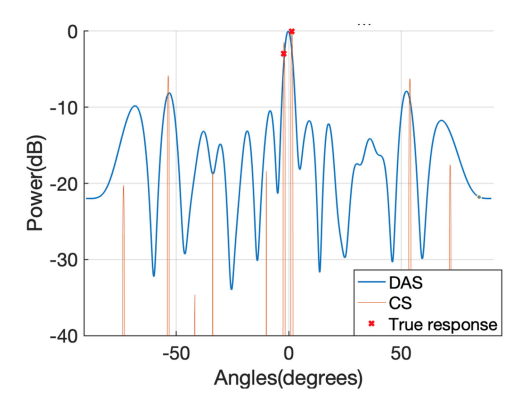


FIGURE 13. Final measurement for two targets spaced at 2 degrees apart, comparing delay-and-sum (DAS), CS, and the true target response.

was only able to resolve targets 4° apart in the best case (see [17, Table 1 and Fig. 26]) by applying delay and sum (DAS) beamforming only.

For the radar system proposed in this paper, detection and estimation has been performed with two methods, DAS and YALL1-CS, and results are shown in Fig. 13. The two targets being positioned at an angular separation of 2° are not distinguishable with DAS, but they can be clearly identified when applying CS. As expected from the antenna measurements, the SLLs are somewhat high and can lead to false detections in both methods. Also, if a threshold is set at -5 dB since the SLL of the virtual reciever array is also about -5 dB (see Fig. 9), then two targets can be clearly identified using CS, while DAS would only identify one target. On the other hand, a threshold at -10 dB would be unsuitable, as false targets would be identified at $\pm 52^{\circ}$ for both approaches as shown in Fig. 13.

B. SPECTRAL SMOOTHING USING PATTERN MULTIPLICATION

In radar detection, angular target estimates such as the ones processed using digital radar signals are mostly shaped similar to a bell-shaped curve as seen in a normal or Gaussian distribution. Multiplying several Gaussian functions will result in reduction of the pattern level minima (or lowering of the troughs) with respect to the main peak [42], [43], [44]. In this manner, the signal can have an improved SLL response for the radar return. As outlined in [44], this pattern multiplication approach can define a sharper peak for the target estimates and improved radar accuracy. More information about this smoothing process, pattern sharpness, and the underlying mathematics can be found in [45]. Practically, the technique is basically related to the averaging of multiple frequency-domain samples when completing VNA measurements for low power signals in a noisy environment (and this can improve the accuracy of the recorded data). This can result in a cleaner or more accurate target estimate response for the radar where the noise level

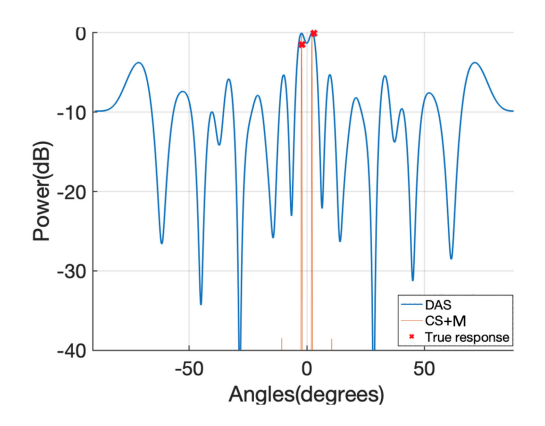


FIGURE 14. Final measurement for two targets spaced at 2 degrees apart, comparing DAS and CS with multiplication (CS+M).

is effectively reduced, making for an improved signal-tonoise-ratio (SNR).

This pattern multiplication method [44] is also based on multiple readings of the same target scenario which can be used to reduce the SLL. As mentioned above, this technique can improve the SNR for the target estimate response mainly due to this pattern multiplication operation and this methodology is applied here for the CS results, mainly, to reduce false reconstructions (which are observed in Fig. 13, for example at about $\pm 52^{\circ}$ away from broadside). By adding this technique, the target detection response is improved as can be seen in Fig. 14, with false detections 40 dB lower than the response of the actual targets. This is very helpful in situations where clutter would hinder radar performance, however, as it is noted in [44], the approach does not increase angular resolution. Regardless, the combination of CS and multiplication yields a clearer image for the detection of two targets with just 2° separation.

It should also be mentioned that simple computing hardware was employed for the data processing and the SPP; performed using a laptop running MATLAB. In particular, the computer characteristics are as follows: Intel Core i7 CPU (3.60 GHz, 4 cores, and 8 logical processors), and 16 GB of RAM. Moreover, the computation time was calculated as about 35 milliseconds (or less) and it is expected that this can be improved if the system is transitioned to FPGA-based processing. Similar computing times were observed as reported in [17] and [43] using analogous computation hardware, which was considered acceptable for development automotive radar setups and the related target tracking scenarios.

VI. CONCLUSION

A microwave/millimeter-wave FMCW digital radar system is presented in this paper, in the context of automotive radar collision avoidance scenarios. The paper also demonstrates how an SIW sparse array can aid radar detection by offering an enlarged MIMO virtual antenna aperture using sparse signal processing, while preserving an acceptable SLL response and competitive receiver bandwidth of 6.25%.

The radar signal processing consists of applying sparsereconstruction techniques of the digital radar channels and spectral smoothing. In this way, targets at an angular separation of just 2° were shown to be distinguishable during trial measurements in an anechoic chamber, and the developed receiver offers a 33% reduction when compared to an equivalent ULA. Findings in the paper are also compared with other radar systems present in the literature (see Table I), identifying system characteristics such as angular resolution and receiver percentage bandwidth. As can be observed, advancements offered by the proposed radar system include planar antenna implementation as well as improved system bandwidth and angular resolution.

The paper also discussed the methodology of obtaining a sparse antenna array design, given some constraints, such as antenna inter-element spacing and the number of elements. Configurations have been compared for best possible radar angular resolution and SLL, prior to fabrication of the new radar antenna. Also, good agreement between simulations and measurements have been reported. Future work can include achieving better SLL responses for the antenna design by tapering for non-broadside scenarios while also considering radar systems with bandwidths in excess of 7% and higher carrier frequencies.

ACKNOWLEDGMENT

The authors would like to thank the European Microwave Association (EuMA) for organising the EuMA Internship 2020 and the host, TNO, for providing the measurement facilities to complete this work. The authors would like to indicate that the work is only the author's views, and that The Horizon 2020 Agency is not responsible for any information contained in the paper.

REFERENCES

- C. Malaquin, "Automated driving: Market perspective for radar," in Proc. Eur. Microw. Week Automot. Forum, 2021, pp. 1–59.
- [2] C. Waldschmidt, J. Hasch, and W. Menzel, "Automotive radar— From first efforts to future systems," *IEEE J. Microw.*, vol. 1, no. 1, pp. 135–148, Jan. 2021.
- [3] S. Sun and Y. D. Zhang, "4D automotive radar sensing for autonomous vehicles: A sparsity-oriented approach," *IEEE J. Sel. Topics Signal Process.*, vol. 15, no. 4, pp. 879–891, Jun. 2021.
- [4] D. Mateos-Núñez, M. A. González-Huici, R. Simoni, F. B. Khalid, M. Eschbaumer, and A. Roger, "Sparse array design for automotive MIMO radar," in *Proc. 16th Eur. Radar Conf. (EuRAD)*, 2019, pp. 249–252.
- [5] A. Correas-Serrano and M. A. González-Huici, "Experimental evaluation of compressive sensing for DoA estimation in automotive radar," in *Proc. 19th Int. Radar Symp. (IRS)*, 2018, pp. 1–10.
- [6] S. Nagesh, J. Ender, and M. A. González-Huici, "Array position optimisation for compressed sensing MIMO radar based on mutual coherence minimisation," in *Proc. 23rd Int. Radar Symp. (IRS)*, 2022, pp. 98–103.
- [7] D. Phippen, L. Daniel, E. Hoare, M. Cherniakov, and M. Gashinova, "Compressive sensing for automotive 300 GHz 3D imaging radar," in *Proc. IEEE Radar Conf. (RadarConf)*, 2020, pp. 1–6.
- [8] C. Kurtscheid and M. A. Gonzalez-Huici, "Design of a fixed aperture 2D sparse radar array," in *Proc. 21st Eur. Radar Conf. (EuRAD)*, 2024, pp. 111–114.
- [9] D. Schwarz, M. Linder, C. Bonfert, and C. Waldschmidt, "Improving the image quality in high-resolution 4D radars with sparse arrays by compressed sensing," in *Proc. Int. Conf. Electromagn. Adv. Appl.* (ICEAA), 2023, pp. 122–127.

- [10] L. Anitori, A. Maleki, M. Otten, R. G. Baraniuk, and P. Hoogeboom, "Design and analysis of compressed sensing radar detectors," *IEEE Trans. Signal Process.*, vol. 61, no. 4, pp. 813–827, Feb. 2013.
- [11] D. J. Bekers et al., "On pre-whitening and accuracy in DOA estimation by sparse signal processing on beamformed data," in *Proc. 4th Int. Workshop Compressed Sens. Radar, Sonar, Remote Sens. (CoSeRa)*, 2016, pp. 202–206.
- [12] L. Anitori and A. Maleki, "4 compressed CFAR techniques," in Compressed Sensing in Radar Signal Processing. Cambridge, U.K.: Cambridge Univ. Press, 2019, p. 105.
- [13] C. J. Baker and A. L. Hume, "Netted radar sensing," *IEEE Aerosp. Electron. Syst. Mag.*, vol. 18, no. 2, pp. 3–6, Feb. 2003.
- [14] C. Shi, L. Ding, F. Wang, S. Salous, and J. Zhou, "Joint target assignment and resource optimization framework for multitarget tracking in phased array radar network," *IEEE Syst. J.*, vol. 15, no. 3, pp. 4379–4390, Sep. 2021.
- [15] B. K. Chalise, D. M. Wong, K. T. Wagner, and M. G. Amin, "Enhancing distributed radar detection performance with reliable communications," *IEEE Trans. Aerosp. Electron. Syst.*, vol. 59, no. 4, pp. 4118–4133, Aug. 2023.
- [16] B. K. Chalise, D. M. Wong, M. G. Amin, A. F. Martone, and B. H. Kirk, "Detection, mode selection, and parameter estimation in distributed radar networks: Algorithms and implementation challenges," *IEEE Aerosp. Electron. Syst. Mag.*, vol. 37, no. 11, pp. 4–22, Nov. 2022.
- [17] C. A. Alistarh et al., "Sectorized FMCW MIMO radar by modular design with non-uniform sparse arrays," *IEEE J. Microw.*, vol. 2, no. 3, pp. 442–460, Jul. 2022.
- [18] C. Alistarh, "Millimetre-wave radar development for high resolution detection," Ph.D. dissertation, School Eng. Phys. Sci., Univ. Edinburgh Heriot-Watt Univ., Edinburgh, Scotland, 2022.
- [19] F. Belfiori, N. Maas, P. Hoogeboom, and W. van Rossum, "TDMA X-band FMCW MIMO radar for short range surveillance applications," in *Proc. 5th Eur. Conf. Antennas Propag. (EUCAP)*, 2011, pp. 483–487.
- [20] F. Roos et al., "Compressed sensing based single snapshot DOA estimation for sparse MIMO radar arrays," in *Proc. 12th German Microw. Conf. (GeMiC)*, 2019, pp. 75–78.
- [21] F. Belfiori, L. Anitori, W. van Rossum, M. Otten, and P. Hoogeboom, "Digital beam forming and compressive sensing based DOA estimation in MIMO arrays," in *Proc. 8th Eur. Radar Conf.*, 2011, pp. 285–288.
- [22] A. Dürr et al., "On the calibration of mm-Wave MIMO radars using sparse antenna arrays for DoA estimation," in *Proc. 16th Eur. Radar Conf. (EuRAD)*, 2019, pp. 349–352.
- [23] J.-J. Fuchs, "Detection and estimation of superimposed signals," in *Proc. IEEE Int. Conf. Acoust., Speech, Signal Process.*, 1998, pp. 1649–1652.
- [24] Y. Zhang, S. Gao, M. Liu, B. Zhang, and Y. Wu, "Phase transition analysis for compressive sensing based DoA estimation in automotive radar," in *Proc. 21st Int. Radar Symp. (IRS)*, 2020, pp. 396–401.
- [25] M. F. Minner, "Compressive sensing applied to MIMO radar and sparse disjoint scenes," Ph.D. dissertation, Dept. Math. Drexel Univ., Philadelphia, PA, USA, 2016.
- [26] J. Yang and Y. Zhang, "Alternating direction algorithms for ℓ₁-problems in compressive sensing," SIAM J. Sci. Comput., vol. 33, no. 1, pp. 250–278, 2011.
- [27] R. Glowinski and A. Marroco, "Sur l'approximation, par elements finis d'ordre un, et la resolution, par penalisation-dualite d'une classe de problemes de dirichlet non lineaires," *Modelisation Mathematique* et Analyse Numerique, vol. 9, no. R2, pp. 41–76, 1975.
- [28] D. Gabay and B. Mercier, "A dual algorithm for the solution of non-linear variational problems via finite element approximation," *Comput. Math. Appl.*, vol. 2, no. 1, pp. 17–40, 1976.
- [29] Y. Zhang, J. Yang, and W. Yin, "User's guide for YALL1—Your algorithms for L1 optimization," Dept. CAAM, Rice Univ., Houston, TX, USA, Rep. TR-09-17, 2010.
- [30] M. Chang, L.-H. Lin, J. Romberg, and A. Raychowdhury, "OPTIMO: A 65-nm 279-GOPS/W 16-b programmable spatial-array processor with on-chip network for solving distributed optimizations via the alternating direction method of multipliers," *IEEE J. Solid-State Circuits*, vol. 55, no. 3, pp. 629–638, Mar. 2020.
- [31] C. Alistarh, L. Anitori, W. van Rossum, S. K. Podilchak, J. Thompson, and M. Sellathurai, "Compressed sensing for MIMO radar using SIW antennas for high resolution detection," in *Proc. 51st Eur. Microw.* Conf., 2022, pp. 1–4.

- [32] C. Alistarh et al., "Millimetre-wave FMCW MIMO radar system development using broadband SIW antennas," in *Proc. 12th Eur. Conf.* Antennas Propag. (EUCAP), 2018, pp. 1–5.
- Antennas Propag. (EUCAP), 2018, pp. 1–5.
 [33] Y. Chong and D. Wenbin, "Microstrip series fed antenna array for millimeter wave automotive radar applications," in Proc. IEEE MTT-S IMWS, Oct. 2012, pp. 1–3.
- [34] Y. Dong and T. Itoh, "Planar ultra-wideband antennas in Ku-and K-band for pattern or polarization diversity applications," *IEEE Trans. Antennas Propag.*, vol. 60, no. 6, pp. 2886–2895, Jun. 2012.
- Antennas Propag., vol. 60, no. 6, pp. 2886–2895, Jun. 2012.
 [35] L. S. Locke, J. Bornemann, and S. Claude, "Substrate integrated waveguide-fed tapered slot antenna with smooth performance characteristics over an ultra-wide bandwidth," Appl. Comput. Electromagn. Soc. J., vol. 28, no. 5, pp. 454–462, 2013.
- [36] K. Wu, M. Bozzi, and N. J. Fonseca, "Substrate integrated transmission lines: Review and applications," *IEEE J. Microw.*, vol. 1, no. 1, pp. 345–363, Jan. 2021.
- [37] R. Garg, I. Bahl, and M. Bozzi, Microstrip Lines and Slotlines. Norwood, MA, USA: Artech House, 2013.
- [38] F. Xu and K. Wu, "Guided-wave and leakage characteristics of substrate integrated waveguide," *IEEE Trans. Microw. Theory Techn.*, vol. 53, no. 1, pp. 66–73, Jan. 2005.
- [39] T. A. Milligan, Modern Antenna Design. Hoboken, NJ, USA: Wiley, 2005.
- [40] R. Garg, Microstrip Antenna Design Handbook. Norwood, MA, USA: Artech House, 2001.
- [41] S. K. Podilchak, P. Baccarelli, P. Burghignoli, A. P. Freundorfer, and Y. M. M. Antar, "Analysis and design of annular microstrip-based planar periodic leaky-wave antennas," *IEEE Trans. Antennas Propag.*, vol. 62, no. 6, pp. 2978–2991, Jun. 2014.
- [42] C. A. Alistarh, S. K. Podilchak, G. Goussestis, J. S. Thompson, and J. Lee, "Spectral smoothing by multiple radar pattern multiplication for improved accuracy," in *Proc. 18th Int. Symp. Antenna Technol.* Appl. Electromagn. (ANTEM), 2018, pp. 1–2.
- [43] P. D. Hilario Re et al., "FMCW radar with enhanced resolution and processing time by beam switching," *IEEE Open J. Antennas Propag.*, vol. 2, pp. 882–896, 2021.
- [44] C. A. Alistarh, S. K. Podilchak, J. Thompson, and M. Sellathurai, "Radar accuracy improvement by pattern multiplication for automotive radar systems and other sensing scenarios," in *Proc. Int. Conf. Radar Syst. (RADAR)*, 2022, pp. 232–236.
 [45] J. K. Kauppinen, D. J. Moffatt, H. H. Mantsch, and D. G. Cameron,
- [45] J. K. Kauppinen, D. J. Moffatt, H. H. Mantsch, and D. G. Cameron, "Smoothing of spectral data in the Fourier domain," *Appl. Opt.*, vol. 21, no. 10, pp. 1866–1872, 1982.



CRISTIAN A. ALISTARH (Member, IEEE) received the M.Eng. degree in electronics and computer science from The University of Edinburgh, Edinburgh, U.K., in 2015, as a Keycom Scholar, and the joint M.Sc. degree in sensors and imaging systems from the University of Glasgow, Glasgow, U.K., and the University of Edinburgh, and the Ph.D. degree with Heriot-Watt University, Edinburgh, U.K. together with the University of Edinburgh in partnership with Samsung Research and Development, South Korea, in 2022. His

research interests include satellite systems, passive component design, high resolution automotive radar, MIMO systems, digital beamforming, sparse antenna design, and compressed sensing. He was shortlisted for The Best Paper in Antenna Design and Applications at the European Conference in Antennas and Propagation in April 2018 and also he won first place in the Student Paper Competition at the International Symposium on Antenna Technology and Applied Electromagnetics, Waterloo, Canada, August 2018. In 2019, he was awarded the European Microwave Association Internship Award leading to a research placement with TNO Research and Defence in Netherlands, which was completed successfully in September 2020. In 2023, he worked as an R&D Engineer for ALL.Space, Reading, U.K., on the front end development of a dual-band antenna. In 2024 he joined Honeywell Aerospace Technologies (formerly COMDEV U.K.) as an Advanced RF Engineer and is currently working on satellite data links communications. He is a member of IEEE Antennas and Propagation Society, IEEE Microwave Theory and Technology Society, and IEEE Electron Devices Society.



SYMON K. PODILCHAK (Member, IEEE) received the B.A.Sc. degree in Engineering Science from the University of Toronto, Toronto, ON, Canada, in 2005, and the M.A.Sc. and Ph.D. degrees in electrical engineering from Queen's University, Kingston, ON, Canada, in 2008 and 2013, respectively.

From 2013 to 2015, he was an Assistant Professor with Queen's University. In 2015, he joined Heriot-Watt University, Edinburgh, U.K., as an Assistant Professor, and became an Associate

Professor in 2017. He is currently a Senior Lecturer with the School of Engineering, The University of Edinburgh, Edinburgh, U.K. He has had industrial experience as a computer programmer, and has designed 24 and 77 GHz automotive radar systems with Samsung and Magna Electronics. His recent industry experiences also include the design of high frequency surface-wave radar systems, professional software design and implementation for measurements in anechoic chambers for the Canadian Department of National Defense and the SLOWPOKE Nuclear Reactor Facility. He has also designed compact antennas for wideband military communications, highly compact circularly polarized antennas for CubeSats with COM DEV International (now Honeywell) and The European Space Agency (ESA), and new wireless power transmission systems for Samsung. His research interests include surface waves, leakywave antennas, metasurfaces, UWB antennas, phased array antenna systems, and RF integrated circuits.

Dr. Podilchak has been the recipient of many best paper awards and scholarships, most notably Research Fellowships from the IEEE Antennas and Propagation Society, IEEE Microwave Theory and Techniques Society, and five Young Scientist Awards from the International Union of Radio Science. He was a recipient of a Fellowship from the Natural Sciences and Engineering Research Council of Canada (NSERC). In 2012, he received the Best Paper Prize for Antenna Design at the European Conference on Antennas and Propagation for his work on CubeSat antennas, and in 2016, European Microwave Prize for his research on surface waves and leaky-wave antennas. He was bestowed a Visiting Professorship Award at Sapienza University, Rome, Italy, in 2017 and 2019, respectively, and from 2016 to 2019, his research was supported by a H2020 Marie Sklodowska-Curie European Research Fellowship. He was recognized as an outstanding reviewer of the IEEE Transactions on Antennas and Propagation, in 2014 and 2020. He was also the recipient of the COVID-19 Above and Beyond Medal for leading research on remote microwave sterilization of the coronavirus. He was also the Founder and First Chairman of the IEEE AP-S and IEEE MTT-S Joint Chapters in Kingston, ON Canada, and Scotland, in 2014 and 2019, respectively. In recognition of these services, he was presented with an Outstanding Volunteer Award, and in 2020 and 2021, respectively. IEEE recognized this Scotland Chapter for its activities and it was awarded the winner of the Outstanding Chapter Award hosted by these two IEEE Societies. He was also the recipient of the Outstanding Dissertation Award for his Ph.D. He was a Lecturer with the European School of Antennas and an Associate Editor for the IET Electronics Letters. He was also the Guest Associate Editor of IEEE OPEN JOURNAL OF ANTENNAS AND PROPAGATION and IEEE ANTENNAS AND WIRELESS PROPAGATION LETTERS. He is currently an Associate Editor of the IEEE TRANSACTIONS ON ANTENNAS AND PROPAGATION. He is also a Registered Professional Engineer.



DAVE J. BEKERS (Senior Member, IEEE) received the M.Sc. degree in mathematics and the P.D.Eng. and Ph.D. degrees from the Technische Universiteit Eindhoven, Eindhoven, The Netherlands, in 1999, 2001, and 2004, respectively. He carried out his final project for the post-graduate program "Mathematics for Industry" and the Ph.D. Project in the field of array antennas with Thales Nederland, Hengelo, The Netherlands. Since November 2004, he has been with TNO, The Hague, The Netherlands, organization for applied

scientific research, where he first worked in antenna design, modeling, and simulation, and guided a few projects in the field of mm-wave and THz antenna technology. In the past seven and eight years, he worked mainly in the fields of radar signal processing and phased-array antenna topics, such as beamforming, target detection, parameter estimation, and novel waveforms. Additionally, he had the technical guidance at TNO for a few activities carried out within D-RACE, the Dutch Radar Centre of Expertise, a strategic alliance between TNO and Thales Nederland B.V.



LAURA ANITORI (Senior Member, IEEE) received the Master of Science degree (cum laude) in telecommunication engineering from the University of Pisa, Italy, in 2005 and the Ph.D. degree (cum laude) in electrical engineering from the Technical University of Delft, The Netherlands, in 2013. From 2005 to 2007, she was a Research Assistant with the Telecommunication Engineering Department, Twente University, The Netherlands, where she carried out fundamental research on Importance Sampling for Space Time

Adaptive Processing for radar. Starting in 2007, she was working with the Radar Technology Department of TNO, The Netherlands, where she was a Senior Scientist and a Program Manager of a 4-year Defense funded radar research program. Her work is fully embedded in the "Radar and Integrated Sensor Suite 2030" technology roadmap of the Royal Dutch Navy, which focuses on the development of the radar sensor suite for the next-generation Integrated Air and Missile Defense frigates for the Navy. Programs in this roadmap are carried out in the framework of a strategic alliance between TNO, Thales Netherlands, and the Dutch Ministry of Defense. As one of the main technical advisors and coordinators within this roadmap, she was responsible to identify new radar system concepts and architectures, innovative waveforms, and emerging signal processing algorithms for naval phased array radars and to ensure that these can grow from low to high

She is also deeply involved in the international scientific community to support, promote, and organize new and existing activities. Since 2017, she has been a member of the IEEE AESS Radar System Panel, where she is a Vice Chair of the Student Competition Committee. She is a member of the European Microwave Association and its Young Professional Team, which promotes and supports young graduate students to the microwave

She has written numerous highly cited journal and conference papers. She is also a Reviewer for several journals and was an Associate Editor of the IEEE SENSOR JOURNAL from 2018 to 2019. She serves on several technical program committees and student competition committees at international conferences (IEEE International Radar Conferences, CoSeRA Workshops, SSPD, European Microwave Week, IRS). She is an active member of NATO's Sensors and Electronics Technology (SET) Panel. She initiated and chaired several activities in the panel, and she is currently director of SET Lecture Series on "Compressive Sensing Techniques for Radar and ESM Applications" and chair of the research task group on "Integrating Compressive Sensing and Machine Learning Techniques for Radar Applications". Her significant contributions to the SET Panel were recognized with NATO's Early Career Award in 2018. The Task Group SET-236 that she chaired from 2016 to 2019 also received the 2019 SET Panel Excellence Award. Since January 2024, she has been with the CNIT Radar and Surveillance Systems National Laboratory, Italy, as Head of Research.



WIM L. VAN ROSSUM received the Ph.D. degree in high energy physics from the University of Utrecht, Utrecht, The Netherlands, in 1998. He has been employed with the Netherlands Organization for Applied Physics, TNO since 1998. He is currently working at TNO Defence, Security and Safety at The Hague, The Netherlands, where he is involved in developing new radar concepts utilizing irregular waveforms with the corresponding novel signal processing.



ROB BOEKEMA was born in Maassluis, The Netherlands, in 1962. He received the B.Sc. degree in information technology from HTS Rijswijk, Rijswijk, The Netherlands, in 1985. After fulfilling his service in the Dutch Army, he joined the TNO Physics and Electronics Laboratory, The Hague, The Netherlands, in 1987, where he started working in the research on radar propagation above sea. Since 2000, he has been involved in the design and implementation of radar performance computer models. Since 2017, he has been responsible for

the anechoic chamber and near field facilities with TNO, where antenna characterization and radar cross section (RCS) measurements are performed.



IRAM SHAHZADI (Student Member, IEEE) received the B.Sc. and M.Sc. degrees in electrical engineering from the University of Engineering and Technology, Lahore, in 2015 and 2018, respectively, and the Ph.D. degree from the University of Edinburgh in 2025, specializing in dual-polarized antenna design with high isolation levels for full-duplex communication systems, FMCWradar, and antenna and solar cell integration. Her research focuses on developing innovative antenna solutions to enhance wireless

communications, radar sensing, and energy-harvesting technologies.



MATHINI SELLATHURAI (Fellow, IEEE) is currently a Professor of signal processing and wireless communications and the Dean of Science and Engineering with Heriot-Watt University, Edinburgh, U.K. She has been active in signal processing research for the past 20 years and has a strong international track record in wireless communications. She held visiting positions with Bell Laboratories, Holmdel, NJ, USA, and with the Canadian Communications Research Centre, Ottawa, ON, Canada. She has published over 250

peer-reviewed papers in leading international journals and conferences and two research monographs. Her research interests include machine learning and statistical signal processing techniques applied to wireless communications, radar, assistive care, robotics, and hearing aids. She is a recipient of the IEEE Communication Society WIE Mentorship Award in 2022, the Fred W. Ellersick Best Paper Award in 2005, the Industry Canada Public Service Awards in 2005, and the Technology Transfers Awards in 2004. She received the Natural Sciences and Engineering Research Council of Canada Doctoral Award for her Ph.D. Dissertation. She was an Editor of the IEEE TRANSACTIONS OF SIGNAL PROCESSING from 2009 to 2018, the General Chair of IEEE SIGNAL PROCESSING ADVANCES IN WIRELESS COMMUNICATIONS in 2016, and a member of the IEEE SPCOM Technical Committee from 2014 to 2019. She is a member of the IEEE History Committee and Strategic Advisory Team of U.K. Research Council. She is also an Invited Fellow of the Asia-Pacific Artificial Intelligence Association and Women Engineering Society, U.K.



JOHN S. THOMPSON (Fellow, IEEE) currently holds a Personal Chair in Signal Processing and Communications with the School of Engineering, The University of Edinburgh. He currently specializes in antenna array processing, energy-efficient wireless communications and more recently in the application of machine learning to wireless communications. To date, he has published in excess of 500 journal and conference papers on these topics. He is currently an Area Editor of the wireless communications topic in the IEEE

Transactions on Green Communications and Networking. In January 2016, he was elevated to Fellow of the IEEE for research contributions to antenna arrays and multi-hop communications. He was also one of four scientists elevated to Fellow of the European Association for Signal Processing in 2023 for "signal processing advances in multiple antenna and relayed wireless communication systems". In 2024, he was listed as a Highly Cited Researcher by Clarivate.



YAHIA M. M. ANTAR (Life Fellow, IEEE) received the B.Sc. degree (Hons.) in electrical engineering from Alexandria University, Alexandria, Egypt, in 1966, and the M.Sc. and Ph.D. degrees in electrical engineering from the University of Manitoba, Winnipeg, MB, Canada, in 1971 and 1975, respectively. In May 1979, he joined the Division of Canada, Ottawa, ON, Canada. In November 1987, he joined the Department of Electrical and Computer Engineering, Royal Military College of

Canada, Kingston, ON, Canada, where he has been a Professor since 1990. He has authored or co-authored over 200 journal articles, several books, and chapters in books, over 450 refereed conference papers and holds several patents. He was awarded the Royal Military College of Canada "Excellence in Research" Prize in 2003 and the RMCC Class of 1965 Teaching Excellence Award in 2012. In October 2012, he received the Queen's Diamond Jubilee Medal from the Governor-General of Canada in recognition of his contribution to Canada. He was a recipient of the 2014 IEEE Canada RA Fessenden Silver Medal for Ground Breaking Contributions to Electromagnetics and Communications and the 2015 IEEE Canada J. M. Ham Outstanding Engineering Education Award. In May 2015, he received the Royal Military College of Canada Cowan Prize for excellence in research. He was also a recipient of the IEEE AP-S Chen-To-Tai Distinguished Educator Award in 2017. He has supervised and co-supervised over 90 Ph.D. and M.Sc. theses with the Royal Military College of Canada and Queen's University, Kingston, several of which have received the Governor-General of Canada Gold Medal Award, the Outstanding Ph.D. Thesis of the Division of Applied Science, as well as many best paper awards in major international symposia. He served as the Chair for Canadian National Commission, International Union of Radio Science, from 1999 to 2008, Commission B, from 1993 to 1999, and has a cross-appointment at Queen's University, Kingston. In May 2002, he was awarded the Tier 1 Canada Research Chair in electromagnetic engineering which has been renewed in 2016. He was elected by URSI to the Board as the Vice President, in August 2008 and 2014, and to the IEEE Antennas and Propagation (AP-S) AdCom. In 2019, he was elected as the 2020 President-Elect for IEEE AP-S, and served as its President in 2021. He has served as an Associate Editor for many IEEE and IET journals and an IEEE-APS Distinguished Lecturer. He has chaired several national and international conferences, and has given plenary talks at many conferences. He was appointed as a member of the Canadian Defence Advisory Board of the Canadian Department of National Defence, in January 2011. He is a Fellow of the Engineering Institute of Canada and the Electromagnetic Academy. He is also a URSI Fellow. In 1977, he held a Government of Canada Visiting Fellowship at the Communications Research Center, Ottawa.